V. Prodanov and K. Prodanov, "Relationship between time-constants and 3dB cutoff of high-order damped LTI systems", Proc. IEEE 61st International Midwest Symposium on Circuits and Systems, pp. 85-88, Aug. 2018

Relationship Between Time-constants and 3dB Cutoff of High-Order Damped LTI Systems

Vladimir Prodanov
Electrical Engineering Department
California Polytechnic State University
San Luis Obispo, CA, USA

Katherina Prodanov
Mechanical Engineering Department
California Polytechnic State University
San Luis Obispo, CA, USA

Abstract— this paper deals with linear time-invariant (LTI) systems and examines the link between the 3dB cutoff and time-constants. It shows that the cutoff frequency of a low-pass damped network can be estimated from the reciprocal of a *p*-norm calculated from the system's time-constants. Furthermore, to achieve good accuracy the *p* factor must have a fractional value, for example, p = 1.7. Two formulas are derived, and their performance evaluated using Monte Carlo simulations which reveal a sub-3% error for most cases.

Keywords—bandwidth; cutoff frequency; Elmore; delay; norm; risetime; time-constant;

I. INTRODUCTION

This paper discusses the relationship between time-constants and 3dB bandwidth of damped linear time-invariant (LTI) systems. A brief review of the time and frequency domain descriptions of such systems is offered. Then, a comparison between three known methods for estimating the 3dB cutoff is provided. This discussion is important because it frames the rest of the paper.

A. Damped LP Systems in Time and Frequency Domain

Damped low-pass systems are popular because their step response exhibits no overshoot or ringing; a step response with no overshoot implies unipolar impulse response [1].

As captured by (1), the impulse response *h(t)* of a damped low-pass system is the convolution of *n* decaying exponentials. Since the individual exponential functions are non-negative for $t \geq 0$, their convolution, *h(t),* is also non-negative. This is true irrespective of the system order *n* or the values of the time-constants τ_k.

$$h(t) = h(t,\tau_1) * h(t,\tau_2) * \dots * h(t,\tau_n) \tag{1}$$

$$where \quad h(t,\tau_k) = \frac{1}{\tau_k} exp\left(-\frac{t}{\tau_k}\right)$$

Expression (2) captures the frequency-domain behavior of a low-pass damped network. $H(j\omega)$, the Laplace transform of (1) evaluated at $s=j\omega$, is an all-real-pole transfer function. Here a reciprocal relationship holds between the magnitudes of the poles and the system time-constants.

$$H(j\omega) = \prod_k \frac{1}{1 + j\omega/\omega_{pk}} \quad where \ \left|\omega_{pk}\right| = 1/\tau_k \tag{2}$$

B. The 3dB Cutoff of Damped LP Systems

The magnitude of (2) is a monotonically decreasing function of frequency. This implies a unique 3dB cutoff; the ω_{3dB} calculates from (3).

$$|H(j\omega_{3dB})|^2 \equiv \prod_k \frac{1}{1 + \left(\omega_{3dB}/\omega_{pk}\right)^2} = \frac{1}{2} \tag{3}$$

While no closed-form solution of (3) exists, many formulas offer estimates for the ω_{3dB}. Three such formulas are given below [2-6]. Among them, (4) is the simplest and arguably the most intuitive one; it states that the 3dB cutoff frequency is less than the magnitude of the lowest pole frequency.

$$\omega_{3dB} < \min_k \left\{\left|\omega_{pk}\right|\right\} \tag{4}$$

$$\omega_{3dB} \cong 1\bigg/\sqrt{\sum_k \frac{1}{\omega_{pk}^2}} \tag{5}$$

$$\omega_{3dB} \cong 1\bigg/\sum_k \frac{1}{\left|\omega_{pk}\right|} \tag{6}$$

In the context of an amplifier design, the method of open circuit time-constant (OCTC) is often discussed [2-7]. Conspicuously, the OCTC strategy relies upon (6). We note that despite their differences (4), (5) and (6) are closely related. This fact is demonstrated in the following summary.

Expressions (4), (5), and (6) are Reciprocals of L_p norms of $\boldsymbol{\tau}$*.*

This becomes clear when (4), (5), and (6) are recast with time-constants and the resulting sums are compared to (10) where (10) defines an L_p norm [8].

$$\omega_{3dB} < \min_k \left\{\left|\omega_{pk}\right|\right\} = \frac{1}{\max_k \left\{\tau_k\right\}} \equiv \frac{1}{\|\boldsymbol{\tau}\|_\infty} \tag{7}$$

$$\omega_{3dB} \cong 1\bigg/\sqrt{\sum_k \frac{1}{\omega_{pk}^2}} = \frac{1}{\sqrt{\sum_k \tau_k^2}} \equiv \frac{1}{\|\boldsymbol{\tau}\|_2} \tag{8}$$

$$\omega_{3dB} \cong 1 \Big/ \sum_k \frac{1}{|\omega_{pk}|} = \frac{1}{\sum_k \tau_k} \equiv \frac{1}{\|\boldsymbol{\tau}\|_1} \tag{9}$$

$$\|\boldsymbol{\tau}\|_p = \left(\sum_k \tau_k^p\right)^{1/p} \tag{10}$$

Not only (7) but also (8) and (9) are bounds to ω_{3dB}

$$\frac{1}{\|\boldsymbol{\tau}\|_1} < \omega_{3dB} < \frac{1}{\|\boldsymbol{\tau}\|_2} < \frac{1}{\|\boldsymbol{\tau}\|_\infty} \tag{11}$$

Inequality (11) shows that $1/L_2$ is a tighter upper bound than $1/L_\infty$. This is a direct consequence of a key property of norms: a norm with a larger p-factor has a smaller value [8].

Inequality (11) is not new, but not widely known. Since we could not find a complete derivation elsewhere, we offer one in the appendix of this paper.

Under repeated-pole (same τ) conditions the bandwidth estimation accuracy of both (8) and (9) is poor

The comparison of (12) and (13) to the exact value of ω_{3dB} given in (14) proves this point. For large n, (12) severely underestimates the bandwidth while (13) overestimates it by as much as 20%.

$$\frac{1}{\|\boldsymbol{\tau}\|_1} = \frac{1}{n\,\tau} \quad for \quad \tau_1 = \tau_2 = \cdots = \tau_n \equiv \tau \tag{12}$$

$$\frac{1}{\|\boldsymbol{\tau}\|_2} = \frac{1}{\sqrt{n}\,\tau} \quad for \quad \tau_1 = \tau_2 = \cdots = \tau_n \equiv \tau \tag{13}$$

$$\omega_{3dB} = \frac{\sqrt{2^{1/n} - 1}}{\tau} \quad for \quad \tau_1 = \tau_2 = \cdots = \tau_n \equiv \tau \tag{14}$$

The three observations above motivate our search for a $1/L_p$ formula that predicts the ω_{3dB} more accurately than $1/L_1$ and $1/L_2$.

II. FORMULA WITH AN IMPROVED ACCURACY

A. *Derivation*

Inequality (11) suggests that to improve the accuracy of a $1/L_p$ formula one must use a p-factor with a fractional value between 1 and 2. A 'good' value for the p-factor is found by requiring zero error under repeated-pole (same-τ) condition. This requirement is satisfied when (15) is met.

$$\frac{1}{\Big(\underbrace{\tau_1^p + \cdots + \tau_n^p}_{n\,\tau^p}\Big)^{1/p}} = \frac{\sqrt{2^{1/n} - 1}}{\tau} \tag{15}$$

Solving (15) gives the desired optimum p value (16).

$$p_{opt} = -\frac{2}{\log_n\left(2^{\frac{1}{n}} - 1\right)} \tag{16}$$

Despite its complexity, (16) is well behaved. As seen in Figure 1, for n=2 the p factor has a value of approximately 1.57. The value grows slowly with n, asymptotically approaching 2 when n approaches infinity. For most cases in practice the optimum p value would be between 1.6 and 1.8.

B. *Performance*

To confirm the bandwidth modeling capabilities of the proposed inverse-of-norm formula we resort to Monte Carlo simulations. The study carried in MatLab, uses 5,000 randomly generated τ-vectors of length 3,4,5,6, and 7. The vectors define 1,000 systems of 3rd, 4th, 5th, 6th, and 7th order.

The elements of each τ-vector are uncorrelated, random variables with values uniformly distributed between 1 and 20. Hence, the greatest possible pole spread in all cases is 20. The MatLab script determines the exact ω_{3dB} by a half-interval search, calculates the approximate cutoff $\tilde{\omega}_{3dB}$ by evaluating $1/L_p$ with $p=p_{opt}$, and computes the percent error using (17).

$$Error \equiv \frac{\tilde{\omega}_{3dB} - \omega_{3dB}}{\omega_{3dB}} \times 100, \% \tag{17}$$

For a comparison, the same calculations are also performed for three p-factors with fixed values of 1, 1.7, and 2. The data are then processed to extract median, max, and min errors resulting in the plots shown in Figure 2 and Figure 3.

Figure 2 compares the performance of $1/L_1$ and $1/L_2$. The error associated with $1/L_1$ is always negative whereas that associated with $1/L_2$ is always positive. This finding is consistent with (11) which states that $1/L_1$ and $1/L_2$ bound the 3dB cutoff from below and above, respectively. We also see that $1/L_2$ offers a reasonably accurate approximation for the cut-off frequency. The median error is sub-12% while the range is 0 to 16% for all 5,000 cases studied.

As depicted in Figure 3, the percent error is reduced to sub-3.1% by using a fractional p value.

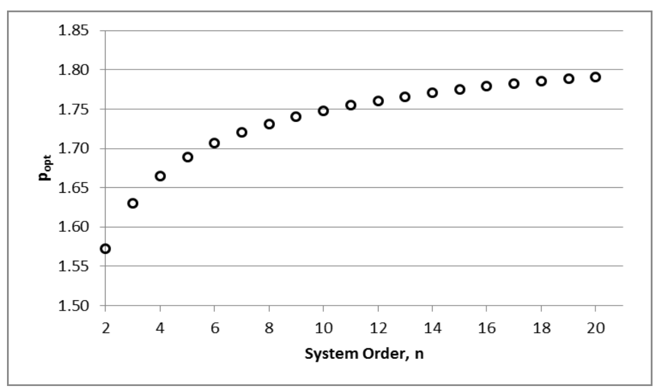

Fig. 1. Depending on system order, the optimum p factor typically ranges from 1.6 to 1.8. To reach a value of 2, n must go to infinity.

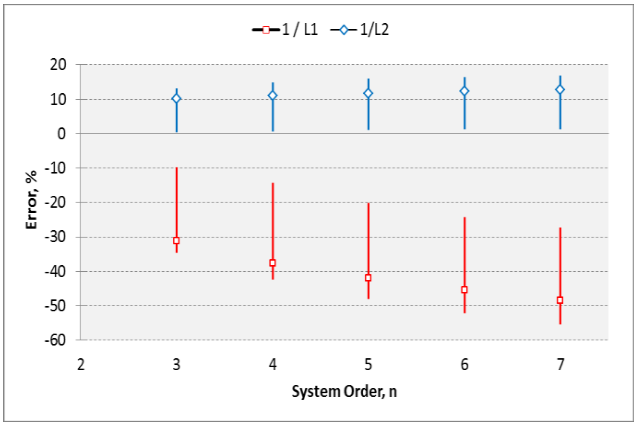

Fig. 2. Bandwidth estimation using 1/L1 and 1/L2. The plot depicts the median value and the range of the percent error.

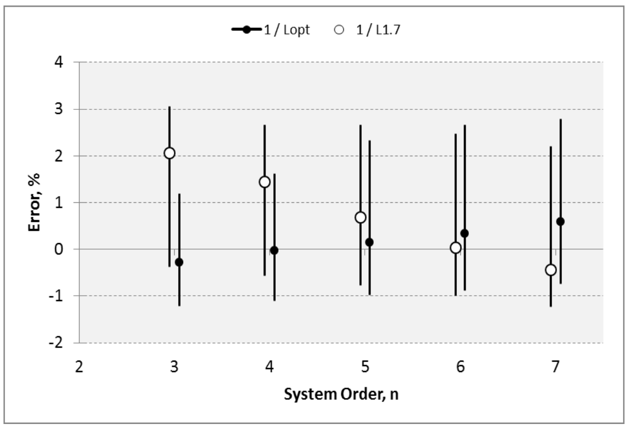

Fig. 3. Bandwidth estimation using 1/Lp with $p=p_{opt}$ and p=1.7.The plot depicts the median value and the range of the percent error.

III. Bandwidth of a Two-Stage Cascade

In the following we derive a formula that calculates the 3dB cutoff of a two-stage cascade from the cut-off frequencies of the individual stages.

Let us assume two damped low-pass systems A and B are connected in a cascade forming system C where the poles (and the time-constants) of C are those of A and B. Further, let us assume that the 3dB frequencies of all three systems calculate with an acceptable accuracy from the same reciprocal-of-norm formula; these assumptions are captured in (18), (19), and (20) where the p factors have the same fixed value p=1.7.

$$\omega_{A,3dB} \cong \frac{1}{\left(\sum_k \tau_{A,k}^{1.7}\right)^{1/1.7}} \tag{18}$$

$$\omega_{B,3dB} \cong \frac{1}{\left(\sum_m \tau_{B,m}^{1.7}\right)^{1/1.7}} \tag{19}$$

$$\omega_{C,3dB} \cong \frac{1}{\left(\sum_k \tau_{A,k}^{1.7} + \sum_m \tau_{B,m}^{1.7}\right)^{1/1.7}} \tag{20}$$

Expression (20) rewrites as (21) and allows us to calculate the 3dB cutoff of the cascade from the cutoff frequencies of the individual stages.

$$\omega_{C,3dB} \cong \frac{\omega_{A,3dB}\,\omega_{B,3dB}}{\left(\omega_{A,3dB}^{1.7} + \omega_{B,3dB}^{1.7}\right)^{1/1.7}} \tag{21}$$

To get an appreciation for (21), consider the following numerical example. One of the stages in a cascade has three poles with magnitudes 1 kHz, 2 kHz, and 3 kHz whereas the other stage has four poles with magnitudes 2.5 kHz, 3 kHz, 5 kHz, and 7 kHz. Unfortunately, none of this information is available to the user; so, they cannot use $1/L_p$ with p determined from (16). In lieu of the complete transfer functions, the cutoff frequencies of the stages, 788 Hz and 1.54 kHz, are provided. Substituting those into (21) produces 669 Hz - an estimate only 2% less than the actual cutoff frequency of 682 Hz. For comparison, $1/L_p$ with $p = p_{opt}$ provides an estimate of 686 Hz and an error of 0.6%, but all the pole information is required.

IV. Significance of L_p Norms of Time-Constants

The reader might wonder about the significance of L_p norms of time constants as related to damped systems: *Do these norms have any physical meaning?* As far as L_1 and L_2 are concerned the answer is affirmative: they are the so-called Elmore delay T_D and Elmore rise-time T_R.

As captured in (22) and (23), T_D and T_R are the first two moments of the system impulse response (1).

$$T_D \stackrel{\text{def}}{=} \int_0^\infty t \times h(t,\boldsymbol{\tau})\, dt = \|\boldsymbol{\tau}\|_1 \tag{22}$$

$$T_R \stackrel{\text{def}}{=} \sqrt{2\pi \int_0^\infty (t - T_D)^2 \times h(t,\boldsymbol{\tau})\, dt} = \|\boldsymbol{\tau}\|_2 \tag{23}$$

Elmore's delay and rise-time are important quantities because they offer a concise description of the system's response to a step input. They also allow the designer to find the T_D and T_R of a cascade from the T_D and T_R of the individual stages [1, 2].

In the context of this paper, (22) and (23) offer an insightful interpretation of (11). The inequality relates three key parameters that reflect the 'speed' of an LTI low-pass circuit – the delay, the rise-time, and the 3dB bandwidth.

Curiously, to obtain the L_1 and the L_2 of a system one need not work in the time domain or carry any integration upon the impulse response. The norms can be read from the denominator coefficients of H(s). For the transfer function (24), $\|\tau\|_1$ equals b_1 and $\|\tau\|_2$ calculates from b_1 and b_2 using (26) [1,2].

$$H(s) = \frac{1}{b_n s^n + \cdots + b_2 s^2 + b_1 s + 1} \tag{24}$$

$$\|\boldsymbol{\tau}\|_1 = b_1 \tag{25}$$

$$\|\boldsymbol{\tau}\|_2 = \sqrt{b_1^2 - 2b_2} \quad (26)$$

Expressions (24), (25), and (26) show that to obtain $\|\boldsymbol{\tau}\|_1$ and $\|\boldsymbol{\tau}\|_2$ one does not have to know the individual time-constants, so it is not necessary to factor the denominator of H(s). This explains the popularity of (5) and (6).

V. Conclusions

Norms, a family of multi-variable functions, offer a convenient way of relating performance specifications of damped systems to time-constants. While Elmore delay and Elmore rise-time calculate from the first two integer norms of $\boldsymbol{\tau}$, capturing the 3dB cutoff requires a fractional L_p norm. Depending on the system order, p-values of 1.6 to 1.8 are required to estimate the 3dB cut-off accurately. We suspect $1/L_p$ formulas with properly selected p factors can estimate other bandwidth specifications, such as the noise bandwidth of a circuit.

Appendix

The decision to explore fractional L_p norms for bandwidth estimation was born out of the observation that the 3dB cutoff of a damped network is bounded by the $1/L_1$ and $1/L_2$. Because of the importance of inequality (11) we include a derivation.

The starting point is (3) which rewrites as (27).

$$\prod_k \left(1 + \left(\frac{\omega_{3dB}}{\omega_{pk}}\right)^2\right) = 2 \quad (27)$$

Taking log-base-10 of both sides changes the product in (27) into a sum and produces (28).

$$\sum_k \frac{\log_{10}\left(1 + \left(\frac{\omega_{3dB}}{\omega_{pk}}\right)^2\right)}{\log_{10}(2)} = 1 \quad (28)$$

According (7) all ratios $|\omega_{3dB}/\omega_{pk}|$ are less than 1. Furthermore, as depicted in Figure 4, over the range 0 to 1, the normalized logarithmic function $\log_{10}(1+x^2)/\log_{10}2$ lays between a line and a parabola. This fact allows us to produce inequality (29) which leads to (30) and (31).

$$\sum_k \left|\frac{\omega_{3dB}}{\omega_{pk}}\right| < 1 < \sum_k \left|\frac{\omega_{3dB}}{\omega_{pk}}\right|^2 \quad (29)$$

$$\|\boldsymbol{\tau}\|_1 \equiv \sum_k \frac{1}{|\omega_{pk}|} < \frac{1}{\omega_{3dB}} \quad (30)$$

$$\frac{1}{\omega_{3dB}} < \sqrt{\sum_k \frac{1}{\omega_{pk}{}^2}} \equiv \|\boldsymbol{\tau}\|_2 \quad (31)$$

An alternative proof of (30) can be found in [9].

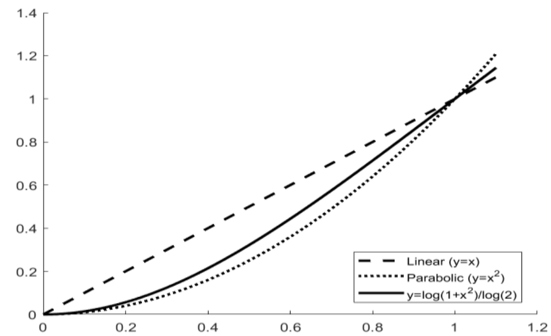

Fig. 4. Over the range x=0-1 the normalized logaritmic function is bounded by a line and a parabola

References

[1] W. C. Elmore, "The transient response of damped linear networks with particular regard to wideband amplifiers," *Journal of Applied Physics*, vol. 19, no. 1, pp. 55–63, Jan. 1948.

[2] T. H. Lee, "Bandwidth estimation techniques," in *The Design of CMOS Radio-Frequency Integrated Circuits,* 2nd ed., New York, NY, USA: Cambridge University Press, 2004, pp. 233- 270.

[3] P. E. Gray and C. L. Searle, "Multistage amplifiers," in *Electronic Principle – Physics, Models, and Circuits,* 1st ed., New York, NY, USA: John Wiley & Sons, 1969, pp. 523- 552.

[4] A. S. Sedra and K. C. Smith, "High-frequency response – general considerations," in *Microelectronic Circuits,* 5th ed., New York, NY, USA: Oxford University Press, 2004, pp. 571-582

[5] R. C. Jaeger and T. N. Blalock, "Amplifier frequency response," in *Microelectronic Circuit Design,* 4th ed., New York, NY, USA: McGraw-Hill, 2011, pp. 1128 – 1193.

[6] S. Salvatori and G. Conte, "On the SCTC-OCTC method for the analysis and design of circuits," *IEEE Tran. Education*, vol. 52, no. 3, pp. 318–327, Aug. 2009.

[7] A. Hajimiri, "Generalized time- and transfer-constant circuit analysis," *IEEE Tran. Circuits and Systems-I: Regular Papers*, vol. 57, no. 6, pp. 1105-1121, June 2010.

[8] C. D. Meyer, "Norms, inner products, and orthogonality," in *Matrix Analysis and Applied Linear Algebra,* 1st ed., Philadelphia, PA, USA: SIAM, 2000, pp. 269-278.

[9] B. Hong and A. Hajimiri, "Upper and lower bounds on a system's bandwidth based on its zero-value time constants," *IET Electronics Letters*, vol. 52, no. 16, pp. 1383-1385, Aug. 2016.